Structural Engineering and Mechanics, *Vol. 69, No. 1 (2019) 69-75*
DOI: https://doi.org/10.12989/sem.2019.69.1.069

Thermal stress analysis around a cavity on a bimetal

Tugba Baytak[a] and Osman Bulut*

Faculty of Civil Engineering, Istanbul Technical University, Buyukdere St., Sarıyer, Istanbul, Turkey

(Received August 6, 2018, Revised November 15, 2018, Accepted November 19, 2018)

Abstract. The plates made of two materials joined to each other having the different coefficient of thermal expansions are frequently encountered in the industrial applications. The stress analysis of these members under the effect of high-temperature variation has great importance in design. In this study, the stress analysis of the experimental model developed for the problem considered here was performed by the method of photothermoelasticity. The thermal strains were formed by the mechanical way and these were fixed by the strain freezing method. For the stress measurements, the method of slicing is applied which provides three-dimensional stress analysis. The analytical solution in the literature was compared with the related stress distribution obtained from the model. Moreover, the axisymmetric finite element model developed for the problem was solved by ABAQUS and the results obtained here compared with those of the experimental model and the analytical solution. As a result of this study, this experimental method and numerical model can be used for these type of thermal stress problems which have not been comprehensively analyzed yet.

Keywords: coefficient of thermal expansion; thermal stress analysis; stress concentration factor; photothermoelasticity; the finite element analysis (FEA)

1. Introduction

The composite materials made of different plates are widely used as the structural members due to their mechanical advantages. Bimetal, which is a type of these materials and may be produced by joining steel and stainless steel elements, have great importance in the industrial structures such as petrochemical process vessels and pressure vessels in reactors. The linear coefficients of thermal expansion of steel and stainless steel are remarkably different. Some defects may occur on the structural members made of bimetal when these are exposed to external effects such as chemical liquids with high pressures (Abdulaliyev *et al.* 2010). Cracks occur around these defects due to the mechanical and thermal effects that change with high gradient. In some cases, the cycles of high-temperature changes lead to brittle fatigue crack of material. Therefore, the precise analyses of thermal stresses around various types of cavities are very important for design so that stress analysis at the tip of a crack can be obtained by an extrapolation on the variation with respect to decreased radius of curvature of the cavity. In addition to this, the location of a cavity should be investigated for this type of material mentioned here.

In technical literature, some stress analyses were performed around cracks using various methods. The theoretical and numerical solutions were developed for the stress analysis around a crack on the plane of interface of two-material composites under thermal effect (Zhao *et al.* 2016, Dang *et al.* 2016). The method of photoelasticity and the finite element method (FEM), which were used here, were also utilized to analyze the stress intensity factor in past works. The stress intensity factor for the crack on the interface of bimetal under transient thermal effect was studied by using the method of photoelasticity (Simon *et al.* 2009). The stress intensity factor for the interface crack under thermal effect was also investigated by the FEM (Ikeda and Sun 2001). There are also some works related to the dynamic behavior of bimaterials. The time-depending stress model of PB-SN solders under cycling loading was developed (Kucukarslan 2003). The method of photoelasticity was also utilized in some recent works. The stress analysis at the tip of a notch at the junction of different materials was performed by photoelasticity (Ayatollahi *et al.* 2011). The stress state was investigated at the tip of a crack in a thin glass plate by dynamic photoelasticity (Sakaue *et al.* 2008). The effect of the welding direction on the stress distribution around the interface of two different materials was cleared by an experimental analysis (Abdulaliyev *et al.* 2007). The change of the thermal stress concentration due to the direction of the cavity near the interface in a plate made of different materials on which the thermal stress was modeled in one direction was obtained by experimental and numerical analyses (Abdulaliyev *et al.* 2012). Because bimetal plate can be considered as a special case of laminated composites or functionally graded materials, this study can be extended to this area using the methods and results obtained here. The stress analysis and optimization for holes with various geometries on laminated composites were performed by using some functions specially defined and FEM (Su *et al.* 2018). The stress field was investigated

*Corresponding author, Ph.D.
E-mail: buluto@itu.edu.tr
[a]Ph.D. Student
E-mail: baytak@itu.edu.tr

 ISSN: 1225-4568 (Print), 1598-6217 (Online)

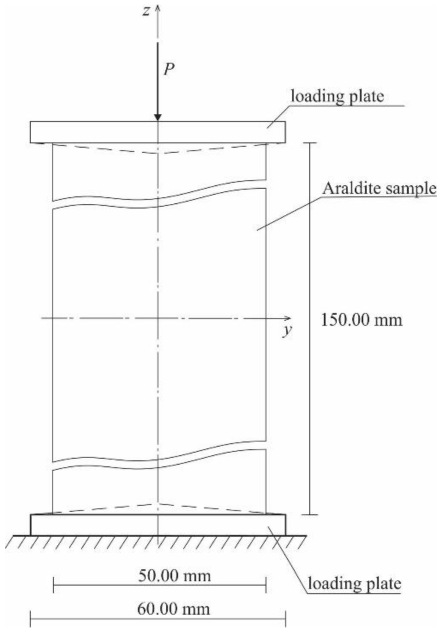

(a) The cylindrical specimen axially loaded

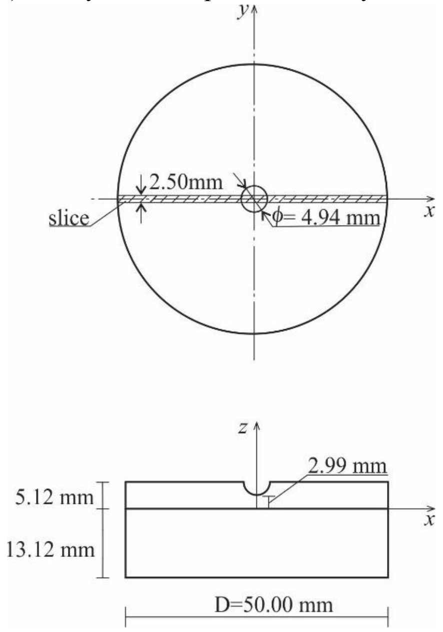

(b) The plan view of the model and the slice taken from the model

Fig. 1 The specimen, the model, and the slice taken from the model

around a rectangular hole on a functionally graded plate (Dave and Dharmendra 2018). A bimetal beam was analyzed for crack propagation under thermal and mechanical loading by FEA (Chama *et al.* 2014). The effect of a uniform temperature loading was investigated for the elasto-plastic stress distributions on a functionally graded material (Demir *et al.* 2017). In case of moving thermal source, the stress distribution on a plate heated from one side was obtained by numerical analysis (Ozisik and Genc 2008). Considering these several works, stress analyses on bimetal plates for a variety of problems must be acquired due to its importance.

In this study, the stress distribution around a cavity that is perpendicular to the interface of the bimetal plate exposed to thermal effect was analyzed by using the method of strain freezing of photothermoelasticity. The type of defect was selected among the cavity types that occur in these type of structures, which were considered in Ref. (Abdulaliyev *et al.* 2010). Abdulaliyev *et al.* (2010) performed an analysis for a similar problem under mechanical effects. The structural element considered here was also analyzed by FEM under thermal effect and the variation of stress concentration factor was obtained with respect to the distance of the cavity tip to the interface and the radius of the cavity tip (Bulut 2018).

In the present work, the experimental model was produced from Araldite, which is an optically sensitive material. Therefore, experimental results obtained here validates the models of FEM and the assumptions of the analytical solutions of these type of problems. The state of strain in the prototype that consists of two materials having different coefficients of thermal expansion under the same temperature change was modeled as the case of a plate made of a single material exposed to two different temperature changes. This analogy is discussed in the literature (Bulut 2018, Bakioglu *et al.* 2011). The strains due to the temperature change were modeled in the related region by mechanical modeling.

The analytical solution of a plate under temperature change, which is expressed by a function varying along the thickness direction, was given by (Timoshenko and Goodier 1970, Boley and Weiner 1997). This solution was verified by the stress data obtained from the corresponding region of the experimental model.

Moreover, the model, which was developed for the problem considered here, was also analyzed by a commercial finite element (FE) package called ABAQUS (Dassault Systèmes, Vélizy-Vilacoublay, France). This numerical solution was verified by using the results obtained from the analytical solution. The results of the experimental and FE analyses around the cavity were compared. They agree well with each other.

This study can be considered as the verification of the experimental and numerical methods in order to extend the work to thermal stress analyzes at the tip of a crack oriented in the perpendicular direction to the interface of bimetal plate and to application of functionally graded materials.

2. The experimental study

The experimental model was made of Araldite that is an optically sensitive material. The material was homogeneous and isotropic and the linear-elastic behavior was considered. The thermal effect generated by a temperature change on the prototype was created by different temperature changes on the model (Bulut 2018, Bakioglu *et al.* 2011). According to this, two different temperature changes were loaded to two regions on a single material of the model, which represent the different materials of the prototype. Because the materials in the prototype have the same material constants except the coefficient of thermal expansion, the state of strain on the prototype due to the difference of this

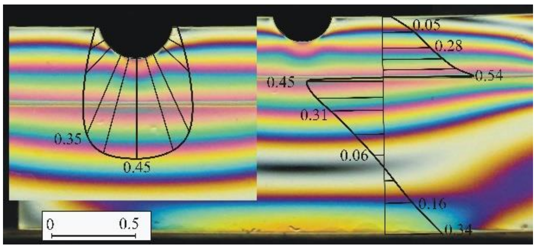

(a) The dimensionless stress distributions near the cavity and along the direction for which the analytical solution was compared

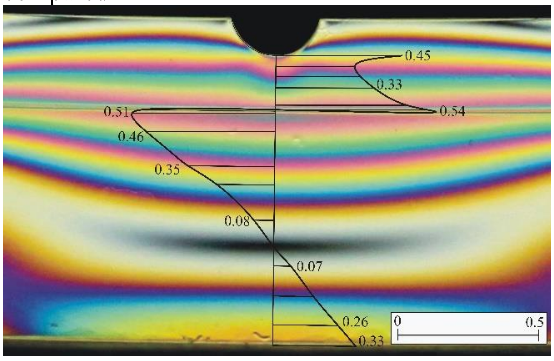

(b) The dimensionless stress distribution along the path starting at the tip of cavity

Fig. 2 The dimensionless stress distributions on the photo of isochromatic fringes obtained from the experiment and the deformed shape of the model

coefficient could be simulated by the difference of temperature change in the experimental model (Frocht 1947, Durelli *et al.* 1958, Timoshenko and Goodier 1970). For simplicity, it was considered that one of this region does not have a temperature change while the other one has a temperature change different from zero. The region of the experimental model having the temperature change was obtained from a cylindrical Araldite specimen, which was prepared in accordance with the photoelastic investigation. The thermal strains on this part were equivalently obtained by the method of mechanical modeling. In order to do this, once the viscoelastic temperature degree of the material was determined as 155ºC, the process of the strain freezing method was applied to the specimen. The sketch and dimensions of the specimen were given in Fig. 1(a). A compressive force of P=1367 N was axially loaded to this specimen and the elastic strains were fixed on it under this effect. This fixing process respectively includes heating the loaded specimen up to the material's viscoelastic temperature determined previously and cooling it to the room temperature with a rate of 5ºC/hour. The uniformly distributed mechanical strains in this specimen were measured using a Mitutoyo digital micrometer as

$$\varepsilon_m = \alpha_m (\Delta T)_m = 0.018 \tag{1}$$

where, the strain ε_m is equated to free thermal expansion value which is calculated by the product of the linear thermal expansion coefficient of the material α_m and the temperature change ΔT_m. As a result of this heating-loading-cooling process, the elastic strains on the specimen were made permanent even if the load is removed.

Measuring the strains of this specimen under compression, the modulus of elasticity of the material was also obtained. Besides, this modulus was obtained by the film tension and 3-P bending tests in a Q800 Dynamic Mechanical Analyzer (DMA) (TA Instruments, New Castle, DE) for the specimens in the convenient dimensions. The mean value of these results gave the modulus of the elasticity of the material at the viscoelastic temperature as follows

$$E_m = 19.3\, MPa \tag{2}$$

The coefficient of optical sensitivity of the material $\sigma_0^{1.0}$ was determined using a disk taken from the same material, which was loaded diametrically by $P_0 = 16.03\, N$. The formula of this coefficient for thin disks was given as follows (Frocht 1947)

$$\sigma_0^{1.0} = \frac{8P_0}{\pi D m} \tag{3}$$

where D represents the diameter of the disk and equals to 50 mm in this study. The photoelastic fringe number at the midpoint of the disk was measured as m=3.581. Substituting this value into the Eq. (3), the coefficient was determined as follows

$$\sigma_0^{1.0} = 0.233 \frac{N}{mm.\, fringe} \tag{4}$$

The part of the model on which the thermal strains were fixed was cut out from the cylindrical specimen by a precise mechanical cutting process. This part was actually a disk with a thickness of 5.12 mm (Fig. 1(b)).

The other part of the model was not under any load and it was also a cylindrical plate with 13.12 mm thickness (Fig. 1b). The diameter of the second part was the same with that of the former one after the strain freezing process.

Two obtained parts were glued to each other by a specific process. During this process, the adhesive is applied as a very thin layer so that the strain at the interface coming from one part will be entirely transferred to the other one. The adhesive was obtained by mixing the epoxy resin and the hardener in a specific ratio and it was applied to the interfaces, homogeneously. The model, which was obtained by the mentioned way, was exposed to the heating-cooling process at the same regime with the method aforementioned. As a result of the first step of this process, the state of strains initially frozen in one part became active in the model and it produced a new distribution. In the second step, the cooling step, the final state of strains was fixed in the model. This also represents a stress distribution, which represents the final state of the thermal stress in the prototype. In order to analyze the stresses around the cavity, a slice with the 2.5 mm thickness was cut out from the model (Fig. 1(b)). This slice was analyzed in the x-z plane, so the photoelastic fringe patterns, which are the results of the thermal stresses modeled by the mechanical loading, were determined along the z-axis and around the cavity. For this aim, the Berek compensator mounted in a polarization microscope Leica DM 4500 P was used. At each specified point, the number of the fringe pattern was obtained by means of a sufficient number of measurements. The obtained fringe numbers were used in the equation (Frocht 1947) given below

$$\left|\sigma_1 - \sigma_2\right| = \frac{m}{t}\sigma_0^{1.0} \tag{5}$$

and the absolute values of the differences of the principle stresses at the corresponding points were calculated. Here, m is the measured number of the fringe pattern, t is the thickness through which the light passes at the measuring point, and σ_1 and σ_2 are the components of the principal stresses. The stress magnitudes obtained by Eq. (5) were converted to dimensionless quantities dividing them to the value given as follows

$$\frac{E_m \alpha_m \left(\Delta T\right)_m}{1-\nu_m} = 0.6948\ MPa \tag{6}$$

which was obtained by the values given in Eqs. (1)-(2). The value of ν_m used in this calculation is the Poisson's ratio of the model's material at viscoelastic temperature and it nearly equals to 0.5. The distributions of the dimensionless quantities, which are so-called as dimensionless stresses, were given in Figs. 2(a)-2(b) along the paths, around the cavity and in two directions of the thickness.

3. The analytical solution

The formula given in the literature for the state of thermal stresses (Timoshenko and Goodier 1970, Boley and Weiner 1997) was used in order to compare the solution with the experimental stress distribution in the corresponding region and to reveal the agreement of the experimental and analytical approach to the problem. This solution was given for the mid-region of a plate with a thickness whose edges are free and the temperature change in this plate is a function of the z-coordinate axis in the thickness direction, that is, T=T(z). Therefore, the expression to be obtained from this solution does not provide the stress distribution in the vicinity of the cavity and edges of the model. However, it was assumed that the distribution of stresses in the model is the same with that obtained by analytical solution in the regions where no discontinuity occurs due to the cavity and edges of the model.

The stress components for the considered case were given as follows (Timoshenko and Goodier 1970, Boley and Weiner 1997)

$$\begin{aligned} &\sigma_{zz} = \sigma_{xz} = \sigma_{yx} = \sigma_{zy} = 0, \\ &\sigma_{xx} = \sigma_{yy} = \frac{\alpha E}{1-\nu}\left\{-T + C_1 + C_2 z\right\} \end{aligned} \tag{7}$$

Here, C_1 and C_2 are constants of integration and they are obtained applying the boundary conditions. The cylindrical components of the state of stress can be easily obtained

Table 1 The values of the stress components σ_{rr} obtained by analytical solution

z coordinates	σ_{rr} (MPa)	σ_{rr} (dimensionless)
-13.12	0.2214	0.3187
-10.12	0.0857	0.1233
-7.12	-0.0501	-0.0720
-4.12	-0.1858	-0.2674
-1.12	-0.3215	-0.4627
0	-0.3722	-0.5357
0	0.3090	0.4447
2.12	0.2131	0.3067
2.99	0.1737	0.2500
5.12	0.0774	0.1114

using these Cartesian coordinate components as follows

$$\begin{aligned} &\sigma_{zz} = \sigma_{rz} = \sigma_{r\theta} = \sigma_{z\theta} = 0, \\ &\sigma_{xx} = \sigma_{yy} = \sigma_{rr} = \sigma_{\theta\theta} \end{aligned} \tag{8}$$

The loading conditions of the problem can be written in the form of resultant force and resultant moments as follows

$$\begin{aligned} &\int_{z=-a}^{b} \left(\sigma_{xx}\right) dz = \int_{z=-a}^{b} \left(\sigma_{yy}\right) dz = 0 \\ &\int_{z=-a}^{b} \left(\sigma_{xx} z\right) dz = \int_{z=-a}^{b} \left(\sigma_{yy} z\right) dz = 0 \end{aligned} \tag{9}$$

The temperature function $T(z)$ was defined as a step function in the model, that is,

$$T(z) = \begin{cases} T, & -a \le z \le 0 \\ 0, & 0 \le z \le b \end{cases} \tag{10}$$

Using the Eqs. (7), (9) and (10), the constants of integration were obtained as follows

$$\begin{aligned} &C_1 = \frac{E}{1-\nu} \frac{\left(\dfrac{b^3+a^3}{3}\right)\varphi - \left(\dfrac{b^2-a^2}{2}\right)\psi}{h\left(\dfrac{b^3+a^3}{3}\right) - \left(\dfrac{b^2-a^2}{2}\right)^2}, \\ &C_2 = \frac{E}{1-\nu} \frac{\left(\dfrac{b^2-a^2}{2}\right)\varphi - h\psi}{h\left(\dfrac{b^3+a^3}{3}\right) - \left(\dfrac{b^2-a^2}{2}\right)^2} \end{aligned} \tag{11}$$

Here, h is the total thickness of the plate, i.e., h=a+b, and the symbols are given as follows

$$\varphi = \int_{-a}^{b} \left[\alpha T(z)\right] dz, \quad \psi = \int_{-a}^{b} \left[\alpha T(z) \cdot z\right] dz \tag{12}$$

If the expression for $T(z)$ in Eq. (10) is substituted into the Eq. (12), then one can obtain

$$\varphi = \int_{-a}^{0}(\alpha T)dz + \int_{0}^{b}(0)dz = \alpha T a$$
$$\psi = \int_{-a}^{0}(\alpha T z)dz + \int_{0}^{b}(0 \cdot z)dz = -\frac{\alpha T a^2}{2} \tag{13}$$

When these expressions in Eq. (13) are used in Eq. (11) and obtained results are substituted into Eq. (7), the formula for the stress distribution along the related direction in the model is obtained. The obtained values of the component σ_{rr} were listed in Table 1 and the variation of this stress component, which is divided by the value given in Eq. (6), is shown in Fig. 3(a).

4. The numerical analysis

In this study, the experimental model developed for the prototype was also analyzed by FEM. The model was axisymmetric and the dimensions were determined in accordance with the geometry given in Fig. 1. The modulus of elasticity and Poisson's ratio of the material were given as follows

$$E_m = 19.3MPa,\ \nu_m = 0.5 \tag{14}$$

The numerical model was created as a single material and a static analysis was performed defining a temperature change in the related region. The geometry of the model was a rectangular shape and the only boundary condition was defined in the center edge, about which the model was axisymmetric (Fig. 4(a)). In the numerical model, the linear coefficient of thermal expansion α_{sm} and the uniform temperature change $(\Delta T)_{sm}$ in the region were selected in accordance with the strain value given in Eq. (1). For simplicity in the analysis, these were chosen as follows

$$\alpha_{sm} = (0.018)[1/°C],\ (\Delta T)_{sm} = (-1)[°C] \tag{15}$$

where the minus sign comes from the contraction of the part on which the elongations due to the axial pressure were fixed. This contraction occurred after the heating-cooling process of the model.

The components of stress and strain were resulted in the cylindrical coordinates since the model was defined as axisymmetric.

The FE mesh of the model was produced by using the elements CAX4R (4-node bilinear axisymmetric quadrilateral) and CAX3 (3-node linear axisymmetric triangle) together. The average size of the mesh elements was 0.1 mm. The numbers of the quadrilateral and triangle elements were 47,426 and 448, respectively. The numerical model and the general mesh were given in Fig. 4(a). The mesh density and the number of the elements were determined by using the method of mesh refinement. The convergence of the numerical results to the analytical solution in the corresponding region of the model was used for this refinement (Fig. 3(a)). This comparison should be made along the vertical direction on which no effects of the edges and cavity occur. The stress distribution was investigated and the convenient direction was determined at the point 6.68 mm away from the symmetry axis. This distance value is the same with that of the vertical path in the experimental model in Fig. 2(a). The distribution of the radial stress component obtained from FE analysis was given in Fig. 4(b).

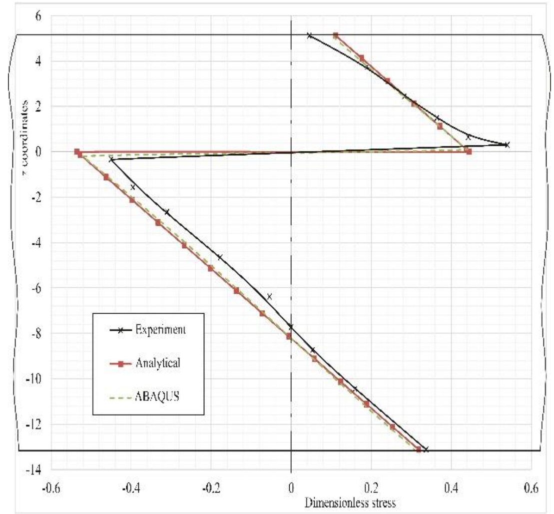

(a) Comparison of the analytical solution and the others in the related region of the model (Fig. 2(a))

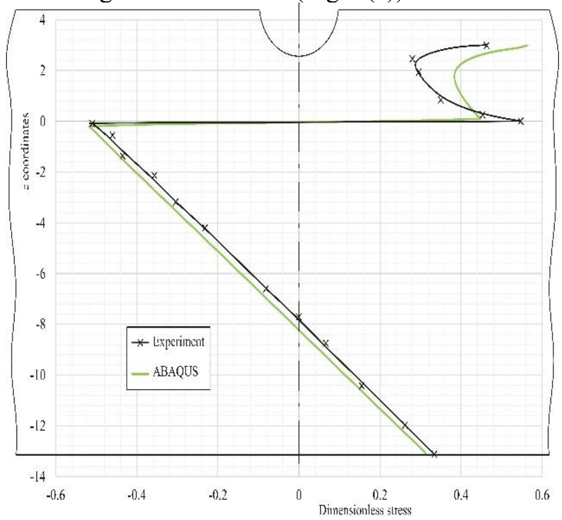

(b) Comparison of the experimental and numerical results on the path in the cavity direction

Fig. 3 The comparison of the results obtained from experimental, analytical and numerical results (the origin of the z coordinates is at the interface)

5. Results

As a result of the experiment in this study, the distribution of isochromatic fringes on the slice was symmetric about the vertical axis passing through the center of the plate. Observing the deformed shape of the model, it can be said that the mechanical behavior under the effect of this temperature change was similar to bending behavior.

In Fig. 3(a), the comparison of the stress distribution obtained from the analytical solution with those of the

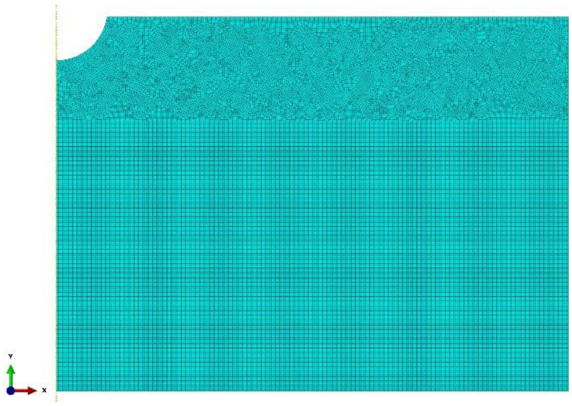

(a) The model and mesh

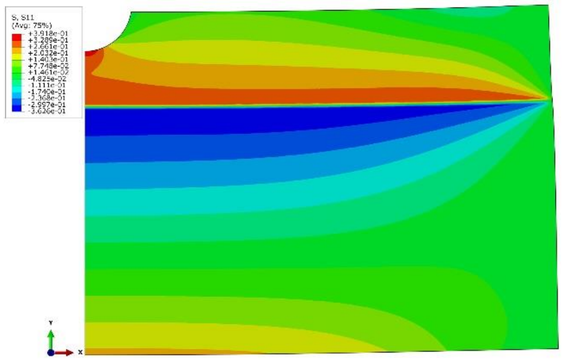

(b) The distribution of the radial stress component obtained from the FE analysis

Fig. 4 The FE model and obtained distribution on the deformed shape.

experiment and numerical analysis were given. These distributions on the path, which has the 6.68 mm distance from the symmetry axis, show that the analytical and numerical results are consistent with those from the experiment.

In Fig. 3(a), the jump value of the distribution of dimensionless stress at the interface was calculated as 0.51+0.49=1.00 along the path, which is not affected by the edges and cavity. This jump was also obtained as 1.00 from the analytical solution. The jump value at the interface for the direction starting from the tip of the cavity equals 0.54+0.51=1.05 (Fig. 3(b)). According to these values, the occurrence of this cavity does not seriously affect the jumping amount at the interface. This value was obtained as 0.97 from the numerical analysis.

In Fig. 3(b), the dimensionless stress value at the tip of the cavity was 0.43 was measured from the experiment. If the analytical solution is used for this point taking z=2.62 mm, then this value is calculated as 0.25. Obviously, this last value of dimensionless stress is at the corresponding point for the same plate with the experimental model but having no cavity. Using these, the stress concentration factor at this point in the model can be calculated as 0.43/0.25=1.72. The dimensionless stress value at the tip of the cavity was obtained as 0.56 from the numerical analysis, so the stress concentration factor calculated from here was 0.56/0.25=2.24. The numerical analysis gave a 24% larger value of the stress concentration factor than that of the experiment. The distributions of the dimensionless stress along the path passing through the tip of the cavity were given in Fig. 3(b) for the results obtained from the experiment and numerical analysis.

The model considered here represents the bimetal plate produced by two plates having different coefficients of thermal expansion. In the model, the dimensionless stress values were obtained at the tip of the cavity and at the interface. In order to calculate the actual stress values at the corresponding points in the prototype, the following formula was used (Frocht 1947, Durelli *et al.* 1958).

$$\sigma_n = \frac{(1-\nu_m)}{(1-\nu_n)} \frac{E_n}{E_m} \kappa \sigma_m \tag{16}$$

Here, the indices m and n indicate the relevant values of the model and prototype, respectively. κ represents the ratio of the free thermal expansion, that is,

$$\kappa = \frac{\varepsilon_n}{\varepsilon_m} = \frac{(\alpha_s - \alpha_{ss})\left(\Delta T\right)_n}{\alpha_m \left(\Delta T\right)_m} \tag{17}$$

where the indices s and ss indicate the constants, which respectively belong to steel and stainless steel. The mechanical properties of the material of the prototype are as follows

$$\begin{aligned} &\alpha_s = (16\times 10^{-6})[1/°C], \alpha_{ss} = (12\times 10^{-6})[1/°C] \\ &E_n = E_s = E_{ss} = 200\times 10^3\, MPa, \nu_n = 0.3 \end{aligned} \tag{18}$$

Using these, the stress value at the tip of the cavity in the prototype that is resulted by the temperature change $\left(\Delta T\right)_n = 200$ °C was calculated as -102.86 MPa.

6. Conclusions

In this study, the state of plane thermal stress was analyzed around a cavity for a plate made of two materials having different coefficients of thermal expansion by the method of photothermoelasticity. The prototype was selected as bimetal plate, which produced by steel and stainless steel. Under the effect of a temperature change, the thermal stress and stress concentration factor were obtained at the tip of the cavity for this plate. The thermal strains obtained by mechanical modeling were fixed in the corresponding region of the model by the strain freezing method, which provides the three-dimensional stress analyses. FEA of the experimental model was also conducted and the results occurred in good agreement.

The analytical solution was compared with the results obtained from the corresponding region of the experimental model. According to this comparison given in Fig. 3(a), the distribution of the experimental measurements is convenient with the linear distribution obtained analytically. The distribution on the same path obtained from the numerical results has good agreement with the others overall.

As an actual problem, the values of stress and stress concentration factor were derived at the tip of the cavity for the change of temperature of 200°C using the experimental measurements. This calculated stress value has an importance in terms of the design of the structural steel members. Another conclusion inferred is that the discontinuity at this location of this cavity has no effect on the jumping value at the interface.

The value of the stress concentration factor obtained from numerical analysis was larger than that of the experiment. This difference may be decreased developing the FE model. A similar case also occurred for the jumping value at the interface on the path passing through the tip of the cavity in the direction of thickness. As a result of a general evaluation, the stress distributions obtained from the numerical and experimental analysis along this path were in good agreement.

In conclusion, it can be stated that the experimental model is convenient to analyze the stress distribution of the plane problem considered in this study. This study contributes the experimental and numerical methods for the thermal stress analysis around the cavity in bimetal to the literature. As a further study, the analysis of the models including cavities in different geometries at different locations will be performed. By this way, developing a comprehensive calculation method for the stress distribution in the bimetal plates due to the thermal effect is aimed.

Acknowledgments

The research described in this paper was financially supported by the Management of Scientific Research Projects of Istanbul Technical University (ITU) (Grant No. 40230) and authors would like to thank the Experimental Mechanics Laboratory (web.itu.edu.tr\mekaniklab).

References

Abdulaliyev, Z., Ataoglu, S., Bulut, O. and Kayali, E.S. (2010), "Three-dimensional stress state around corrosive cavities on pressure vessels", *J. Press. Vess. Technol.*, **132**(2), 021204.

Abdulaliyev, Z., Ataoglu, S. and Guney D. (2007), "Thermal stresses in butt-jointed thick plates from different materials", *Weld. J.*, **86**(7), 201s-204s.

Abdulaliyev, Z., Bakioglu, M., Ataoglu, S., Kurtkaya, Z. and Gulluoglu A.N. (2012), "Thermal stress concentration in plates from different materials", *J. Aircraft*, **49**(3), 941-946.

Ayatollahi, M.R., Mirsayar, M.M. and Dehghany, M. (2011), "Experimental determination of stress field parameters in bi-material notches using photoelasticity", *Mater. Des.*, **32**(10), 4901-4908.

Bakioglu, M., Abdulaliyev, Z., Bulut, O. and Ataoğlu, S. (2011), "Thermal stress intensity factor in plane problems", *Proceedings of the 9th International Fracture Conference*, Istanbul, Turkey, October.

Boley, B.A. and Weiner, J.H. (1997), *Theory of Thermal Stresses*, Dover Publications, New York, U.S.A.

Bulut, O. (2018), "The thermal stress analysis around the cavities in composite plates used for the body of reactors", *J. Fac. Eng. Archit. Gaz.*, **18**(2).

Chama, M., Boutabout, B., Lousdad, A., Bensmain, W. and Bouiadjra, B.A.A. (2014), "Crack propagation and deviation in bi-materials under thermos-mechanical loading", *Struct. Eng. Mech.*, **50**(4), 441-457.

Dang, H.Y., Zhao, M.H., Fan, C.Y. and Chen, Z.T. (2016), "Analysis of an arbitrarily shaped interface crack in a three-dimensional isotropic thermal elastic bi-material. Part 2: Numerical method", *Int. J. Sol. Struct.*, **99**, 48-56.

Dave, J.M. and Dharmendr, S.S. (2018) "Stress field around rectangular hole in functionally graded plate", *Int. J. Mech. Sci.*, **136**, 360-370.

Demir, E., Callioglu, H. and Sayer, M. (2017), "Elasto-plastic thermal stress analysis of functionally graded hyperbolic discs", *Struct. Eng. Mech.*, **62**(5), 587-593.

Durelli, A.J., Phillips, E.A. and Tsao, C.H. (1958), *Introduction to the Theoretical and Experimental Analysis of Stress and Strain*, Mc.Graw-Hill, New York, U.S.A.

Frocht, M.M. (1947), *Photoelasticity*, Wiley, New York, U.S.A.

Ikeda, T. and Sun, C.T. (2001), "Stress intensity factor analysis for an interface crack between dissimilar isotropic materials under thermal stress", *Int. J. Fract.*, **111**(3), 229-249.

Kucukarslan, S. (2003), "The stress model of PB-SN solders", *Sakarya Univ. J. Sci.*, **7**(3), 173-178.

Ozisik, G. and Genc, M.S. (2008), "Temperature and thermal stress distribution in a plate heated from one side surface with a moving heat source", *J. Fac. Eng. Archit. Gaz.*, **23**(3), 601-610.

Sakaue, K., Yoneyama, S., Kikuta, H. and Takashi, M. (2008), "Evaluating crack tip stress field in a thin glass plate under thermal load", *Eng. Fract. Mech.*, **75**(5), 1015-1026.

Simon, B.N., Prasath, R.G.R. and Ramesh, K. (2009), "Transient thermal stress intensity factors of bimaterial interface cracks using refined three-fringe photoelasticity", *J. Strain Anal. Eng. Des.*, **44**(6), 427-438.

Su, Z., Xie, C. and Tang, Y. (2018), "Stress distribution analysis and optimization for composite laminate containing hole of different shapes", *Aerosp. Sci. Technol.*, **76**, 466-470.

Timoshenko, S.P. and Goodier, J.N. (1970), *Theory of Elasticity*, International Edition, McGraw Hill, Singapore.

Zhao, M.H., Dang, H.Y., Fan, C.Y. and Chen, Z.T. (2016), "Analysis of an arbitrarily shaped interface cracks in a three dimensional isotropic thermoelastic bi-material Part 1: Theoretical solution", *Int. J. Sol. Struct.*, **97**, 168-181.

CC